Journal of Ceramic Processing Research. Vol. 4, No. 1, pp. 1~5 (2003)

J O U R N A L O F
Ceramic Processing Research

Processing, characterisation and theory of carbon nanotubes containing SiO_x-based nanocomposites

N. Grobert[a,]*, T. Seeger[b], G. Seifert[c] and M. Rühle[a]

[a]*Max-Planck-Institut für Metallforschung, Ikisekberq sk. 3, 70569 Shuttgar, Germany*
[b]*Instituto de Carboquímica, CSIC, C/ Miguel Luesma Castan, 4, Zaragoza 50015, Spain*
[c]*Institut für Physikalische Chemie und Elektrochemie, Technische Universität Dresden, 01062 Dresden, Germany*

Nanotechnology has become a very popular field for endeavour, embracing biology, chemistry, materials science, engineering, and physics. The interdisciplinary nature of the subject has fostered strong links, opening up new avenues of basic and applied research. Carbon nanotubes (CNTs) have assumed an important role in this context, because of their fascinating chemical and physical properties; thus exhibiting considerable potential for *e.g.* reinforced composites, nanoelectromechanical systems, and numerous other applications. Here we describe a novel route to nanocomposites consisting of multi-walled carbon nanotubes (MWNTs) embedded in amorphous SiO_2. State-of-the-art transmission electron microscopy (HRTEM), electron energy loss spectroscopy (HREELS) and thermal gravimetric analysis (TGA) were used to characterise the material. Based on our observations, we propose theoretical models accounting for stable SiO_x/tube interfaces using density functional based tight binding (DFTB).

Key words: nanotubes, SiO_2, SiO_x, composites, caramic matrix.

Introduction

Carbon nanotubes are excellent candidates for the fabrication of robust composites [1, 2] and conducting polymers [3, 4] due to their fascinating electronic and mechanical properties. For composite applications the formation of a stable tube-matrix interfaces is crucial. However, the surface of MWNTs of large diameter (> 20 nm OD), which exhibit large Young's moduli of *ca*. 1~1.3 TPa [5, 6], tends to be similar to graphite, and chemically 'inert'. Therefore, surface modification treatments are required so that efficient tube-matrix interactions are established. Unfortunately, these treatments can result in extreme degradation of the tubes with a decrease in the Young's modulus, which are responsible for a significantly lower tensile strength of the composites [7].

In this context, the creation of stable nanotube coatings, which do not alter significantly the tube surface, is feasible in order to circumvent this problem. These coated nanotubes are expected to exhibit enhanced mechanical properties when compared to heavily degraded nanotubes. From the chemical point-of-view, MWNTs incorporated into a matrix of a high oxidation resistant material like SiO_2 should reveal a higher oxidation resistance, oxidation being a common drawback of all-carbon materials. Therefore, the synthesis of MWNT/SiO_2 model-composites and thus a detailed theoretical and experimental investigation of the latter is crucial.

Recent work has addressed the formation of irregular metal oxide coatings on MWNTs using single-step chemical routes at low [8, 9] and high temperatures [8, 10]. Here, we report a novel synthesis method to generate bulk nanocomposites consisting of MWNTs embedded in, and coated with SiO_2. The materials were prepared by combining a sonogel technique [11, 12] with a sintering process at high temperatures. For the first time, we studied the tube/matrix interfaces using HRTEM, HREELS and DFTB calculations [13].

Experiments

Composite Synthesis

The MWNT/SiO_x bulk composite was produced as follows: a mixture of 250 mg MWNTs (arc discharge tubes [14]) with 5 g H_2O (pH 2 adjusted with HCl) and 10 g TEOS (molar ratio $nH_2O/nTEOS=6$; total carbon content in the composite: 7.7 wt%) was sonicated using an ultrasonic probe for 5 minutes (SonoPlus with tip KE76, Bandelin, power: 40%), in order to achieve a good tube dispersion in the solution. Subsequently, the gelation process took place in an ultrasonic bath (Bandelin Sonorex RK 100H) for 12 h. For aging, the resulting composite gel was immersed in 10-2 M NaOH for 96 h and dried at room temperature. The composite-gel was then milled using a mortar and a pestle, and compressed uniaxially at 500 MPa (Sack &

*Corresponding author:
Tel : 0049-711-689-3603
Fax: 0049-711-689-3522
E-mail: Grobert@mf.mpg.de

Kiesselbach, Germany). Finally, the pellet was sintered at 1150°C for 15 h in a 300 mbar Ar atmosphere.

Composite Characterisation

Scanning electron microscopy (SEM) was carried out on the fracture surface of the as-produced (dried at room temperature) and the sintered material (1150°C). Transmission electron microscopy (TEM) specimens were prepared from the bulk composite by dimpling and ion-milling (Gatan PIPS Model 591 at 3.8 kV).

TEM was performed using a JEOL 2000 FX operating at 200 kV, HRTEM in a JEOL 4000 EX operating at 400 kV, and EELS using a GATAN DigiPEELS 766 on a dedicated STEM VG HB 501UX operating at 100 kV. Line scans were recorded by rastering the electron beam in a line perpendicular to the tube axis in 2 nm steps, measuring the EEL-spectrum for each step. TGA was performed on a Netzsch STA 409C in air up to a temperature of 1220ºC.

Calculations

In order to understand various interactions and the stability of SiO_x coated tubes, we carried out a series of DFTB calculations on single-wall carbon nanotubes (SWNTs) covered by an individual SiO_x layer. The DFTB method has been described elsewhere [13] and its applicability to the SiC and SiO systems has also been demonstrated [15, 16].

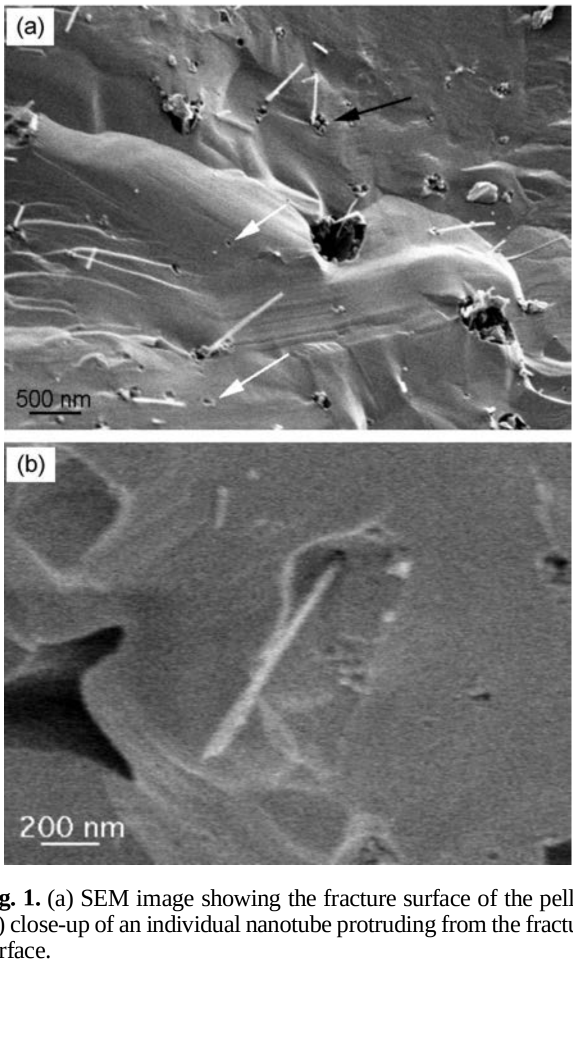

Fig. 1. (a) SEM image showing the fracture surface of the pellet; (b) close-up of an individual nanotube protruding from the fracture surface.

Results and Discussion

The Composite

SEM investigations of the black, brittle and porous granulate material dried at room temperature reveal a distribution of several CNTs and small bundles of CNTs within the fracture surface (Fig. 1a). After sintering the nanotubes are still uniformly distributed, however, it appears that the contact between the CNTs and the matrix is slightly reduced due to a small gap in between the nanotube and the matrix (Fig. 1b). In some cases small holes can be observed, which are due to the removal of CNTs after fracture of the pellet (Fig. 1a).

Figure 2a shows a TEM micrograph of a typical feature found in the composite. The diffraction contrast reveals a MWNT surrounded by a coating. Elemental distribution profiles derived from the EELS line scan analysis across such a structure are shown in Fig. 2b. Silicon and oxygen profiles match and show maxima on both sides of the tubular structure, corresponding to

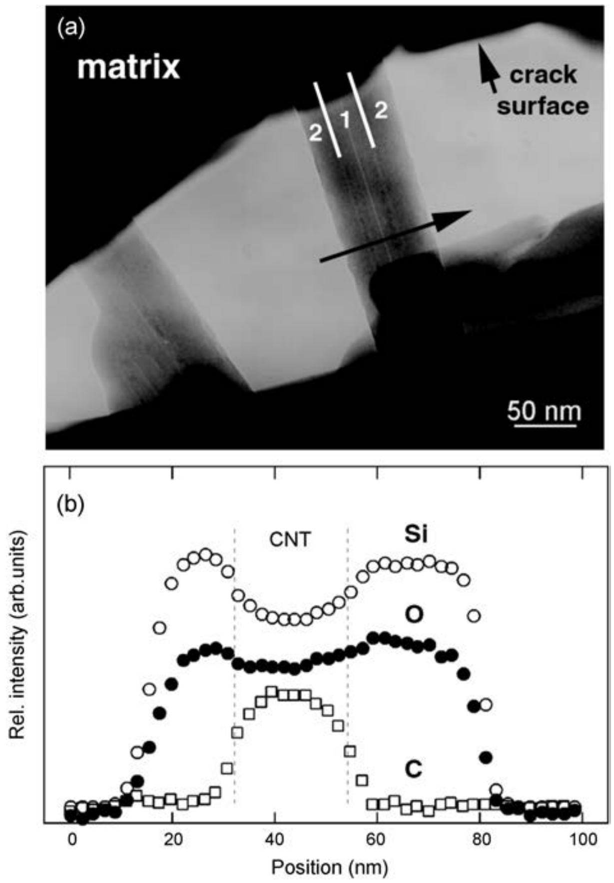

Fig. 2. (a) TEM micrograph of a typical MWNT (1) coated with SiO_2 (2) bridging a crack or pore in the CNT/SiO_2-bulk composite. (b) EELS line scan analysis of a similar structure from for the Si-L, C-K and O-K ionisation edges, indicates that the tubular composite consists of a CNT wrapped by a SiO_2-coating of 20~30 nm thickness.

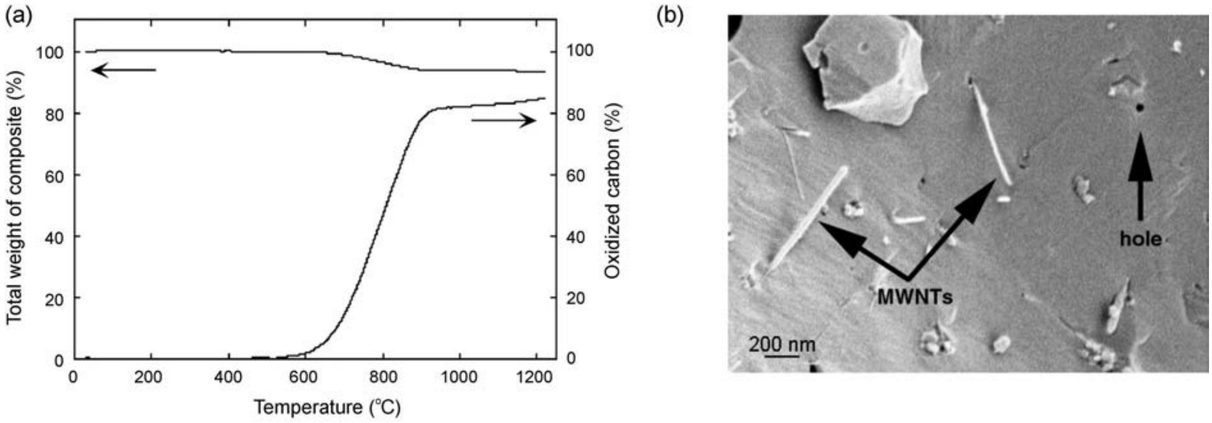

Fig. 3. (a) TGA plot for the MWNT/SiO_2-composite: The upper curve represents the total weight, whereas the other plot represents the carbon-loss relative to the total C-content exhibiting saturation at *ca.* 84%. (b) SEM micrograph of a cracked surface of the MWNT/SiO_2 composite after the TGA measurement (carried out up to 1200°C) of this particular sample. It is noteworthy that the coated tubes have survived oxidation, a fact that is commensurate with the TGA curve.

a SiO_2 coating. The carbon tube intensity dominates the centre of the profile (dashed line). The coating thickness derived from this intensity profile is *ca.* 20~30 nm.

A plot of the TGA of the composite is shown in Fig. 3a. The upper curve represents the total weight of the sample versus the temperature. Since only carbon oxidation can be assumed to take place at the applied temperatures, the total loss of carbon has been calculated which is shown in Fig. 3b. After a high weight-loss at *ca*. 800ºC the curve reaches a saturation at about 84%. This implies that 16% of the carbon remains unoxidised up to the maximum temperature of 1200 ºC. Figure 3b shows an SEM-micrograph of a cracked composite surface after the TGA revealing CNTs that have remained unoxidised. These studies demonstrate that the coated nanotubes are extremely resistant to

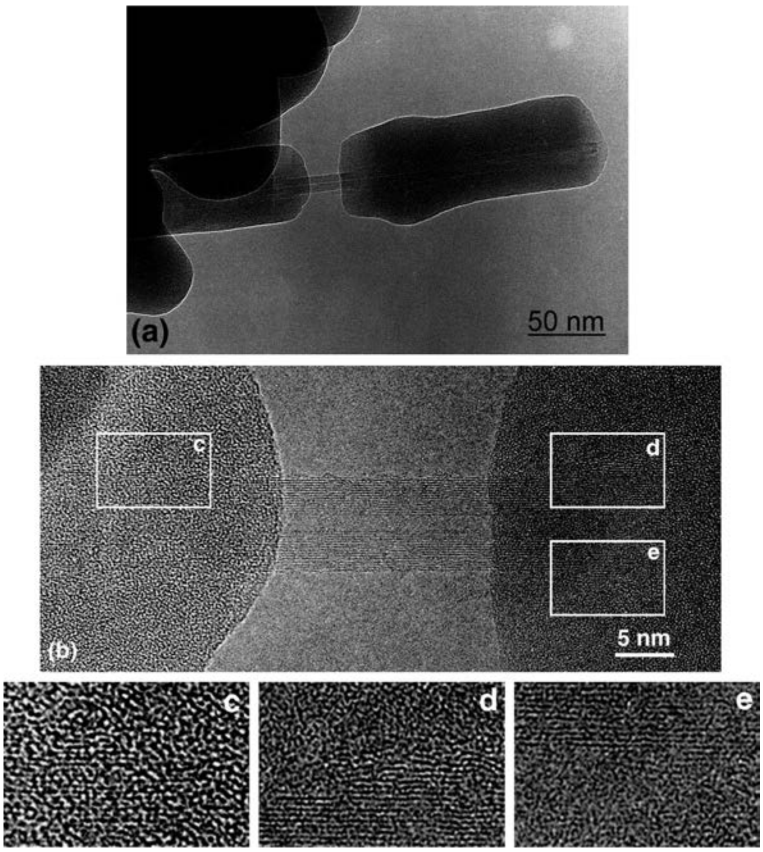

Fig. 4. (a) SiO_x-coated tube produced at 1150°C, which is broken (unusual in our samples). The inner cylinder is composed of a MWNT with 15 undamaged cylinders; (b) magnification of the crack region (as marked in (a)) exhibits broken graphene sheets on the surface of the MWNT (white arrow). The black arrow indicates the proposed slide plane between two cylinders of the tube.

oxidation remaining intact after heating in air up to 1200°C, provided the carbon tubes are completely embedded in the SiO_2 matrix.

A HRTEM image of a cracked SiO_2 coated tube (only observed once in our studies) is depicted in Fig 4a. The broken segments are shifted apart by *ca*. 40 nm and held together by the tube. A magnification of the cracked region (Fig. 4b) reveals an undamaged inner MWNT consisting of 15 concentric carbon cylinders. However, higher magnification of the cracked region at the interface of the tube and the coating (Fig. 4b) reveals heavily damaged outer graphene layers. This suggests that the outer nanotube shells (strongly bonded to the SiO_x matrix) broke apart along the fault of the SiO_x-coating, and slipped off together with the coating. Therefore, we believe that there is a strong bond in the C/SiO_x-interface due to the carbothermal reduction. The sliding took place between the unreacted inner MWNT and the strongly bonded C-SiO_x shell(s).

Calculated Structures

As a first case study we decorated a graphene layer with a SiO_x-monolayer consisting of six-membered SiO_4-rings as shown in Fig. 5. The decoration patterns represent two possible ways of bonding within the CNT/SiO_x interface. In the first case a direct Si-C bond (x=3/2) and in the second case an O-bridged Si-C bond (x=2) is formed. The atomistic geometry of the corresponding structures is depicted in Fig. 6. It is noteworthy

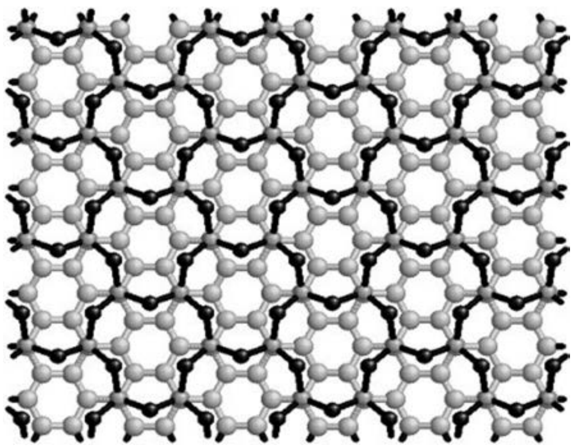

Fig. 5. Top view towards the six-membered SiO_4-rings decorated graphene monolayer.

that the direct Si-C bonded case is spontaneously bending and forming a tubular curvature due to the geometrical mismatch of bonding lengths and the requirement of a Si-O-Si bond angle of about 140°. The O-bridged interface between the silicate layer and the CNT, however, is not stable and the bonds between both layers are spontaneously broken.

Considering these results we conclude that the formation of two possible stable configurations for SiO_x-coated single-walled carbon nanotubes (SWNTs) are feasible. Subsequent studies were carried out on a (20,20) SWNT coated with a SiO_4 tetrahedral cylinder (Fig. 7). Various systems involving the formation of different SiO_x (x=3/2, 2, 5/2) coatings were created. These include: (i) Si-C interactions; (ii) Si-O-C bonds, and (iii) non bonding interactions between the carbon tube and the oxide layer. Therefore the ‘initial-guess’ tubules have been fully relaxed with respect to the atomic positions using conjugate gradient techniques. Dangling bonds on the oxygen atoms were saturated with hydrogen, and periodic boundary conditions were applied along the tube direction.

For stable composite tubes strong interface bonding between the CNT and an inorganic SiO_x matrix needs to be established. The structure shown in Fig. 7a represents the relaxed arrangement for a stable C-SiO_x (x=5/2) composite nanotube containing covalent bonds at the interface. This decoration exhibits six-membered SiO_4 rings within the SiO_x-layer (Fig. 7a). The formation of (Si-C) bonds between the inner and outer tube (Fig. 4a) leads to a partial rehybridization of the carbon atoms ($sp^2 \rightarrow sp^3$). The decoration of this specific SiO_x-layer does not lead to any bonding frustration of carbon atoms (*e.g.* no dangling bonds appear). Instead of possessing a delocalised graphene-like p-electron system, localized benzene-like 6p electron systems are now separated by the sp^3 carbon atoms. Under the condition of preventing bonding frustration other SiO_x decoration patterns also become possible, only if direct Si-C intertubular bonds are formed.

It is important to note that such decorations with SiC bonds, shown in Fig 7a, would be unstable for narrow carbon nanotubes, which exhibit larger curvature. For example stable decoration for a (10,10) carbon nanotube was not observed.

It is noteworthy that as for the planar sheets, the Si-C

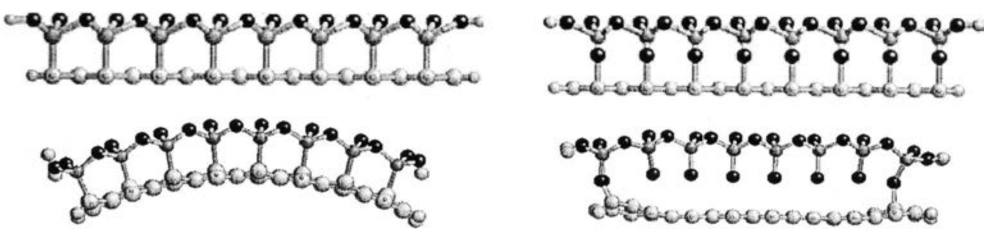

Fig. 6. Illustration of the two structures that occur if the carbon atoms are directly bound to the corresponding silicon atoms a spontaneous bending forming a tubular-like structure occurs (a) or if the carbon atoms are bound to bridging oxygen atoms (b) a separation in two distinct systems (Si-O-C)is observed.

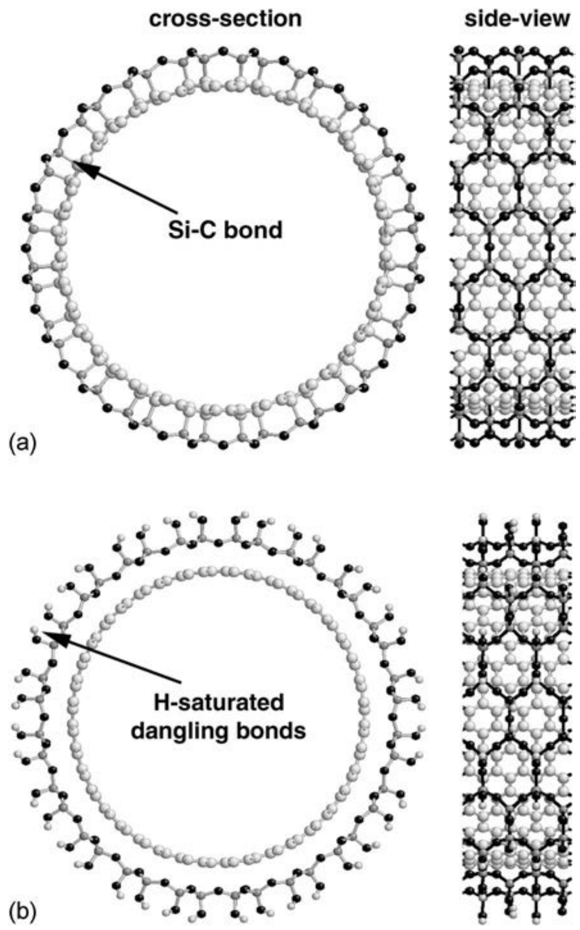

Fig. 7. Molecular models of (20,20) carbon tubules covered by: (a) a cylindrical SiO_x layer (x=5/2) bonded to the carbon tubule via Si-C bridges; (b) a tubular SiO_x layer (x=3/2) without bonding towards the carbon tubule. Here dangling bonds are saturated by H. The O atoms are drawn black. Note the six membered SiO_4 rings on side views.

bonds appear to be the only stable inter-tubular connections and that bonding using Si-O-C bridges does not lead to a stable structure within the SiO_x-layer (when x=2) and the carbon nanotube.

In addition, we also considered a (20,20) carbon nanotube coated with a SiO_x monolayer (x=5/2), which has no bonding interaction between the SiO_x-layer and the carbon tube (Fig. 7b). Interestingly, an individual SiO_x-cylinder without a carbon nanotube in the core is thermodynamically unstable. The latter tends to collapse because the low average coordination number (K<3) is obviously responsible for an insufficient stiffness of the tubular structure. Therefore, the inner carbon tubule stabilises the external constraint of the SiO_x cylinder.

Conclusions

For the first time we were able to characterise the MWNT/matrix interface in an inorganic composite. The composites were fabricated using a novel sol-gel techniques in conjunction with pressure methods and thermal annealing. These materials have proved to be oxidation resistant at temperatures <1200°C. The results widen the horizons of MWNT/matrix interactions, vital for producing MWNT-reinforced composites. For uniform SiO_x coatings, we have proposed that SiO_x can be deposited on MWNTs: (i) by establishing covalent bonds between Si and C, or (ii) without links between the SiO_x shell and the MWNT outer shell. Thus, it should be possible to observe these two types of stable coatings at the SiO_x-MWNT interface of composites, in which the outer most region of the SiO_x coating may well consist of amorphous material (see top in Fig. 3b). We envisage that coated carbon nanotubes with monolayers of different materials will open up a new area of nanotechnology research.

Acknowledgements

We thank U. Salzberger for TEM-specimen preparation. R. Weiland for the TGA measurements. H.-P. Lamparter for X-ray measurements and H. Labitzke for the SEM-investigation and Th. Köhler, Th. Frauenheim fruitful discussions. Financial support is acknowledged from NANOCOMP HPRN-CT-2000-00037 and DFG grant Ru342/11-2.

References

1. M. Terrones, W.K. Hsu, H.W. Kroto, and D.R.M. Walton, Fullerenes and Related Structures; Topics in Chemistry Series, Ed. A. Hirsch (Springer-Verlag); 199 (1998) 189-234.
2. T. Kuzumaki, O. Ujiie, H. Ichinose, and K. Ito, Adv. Eng. Mater. 2 (2000) 416-418.
3. I. Musa, M. Baxendale, G.A.J. Amaratunga, and W. Eccleston, Synthetic Metals 102 (1999) 1250-1250.
4. K. Yoshino, H. Kajii, H. Araki, T. Sonoda, H. Take, and S. Lee, Full. Sci. & Tech. 7 (1999) 695-711.
5. M.J. Treacy, T.W. Ebbesen, and J.M. Gibson, Nature 381 (1996) 678-680.
6. E.W. Wong, P.E. Sheehan, and C.M. Lieber, Science 277 (1997) 1971-1975.
7. P. Calvert, Nature 399 (1999) 210-211.
8. T. Seeger, Ph. Redlich, N. Grobert, M. Terrones, D.R.M. Walton, and H.W. Kroto, Rühle, M.: Chem. Phys. Lett. 339 (2001) 41-46.
9. B.C. Satishkumar, A. Govindaraj, M. Nath, and C.N.R. Rao, J. Mater. Chem. 10 (2000) 2115.
10. B.C. Satishkumar, A. Govindaraj, E.M. Vogl, L. Basumallick, and C.N.R. Rao, J. Mater. Res. 12 (1997) 604.
11. M. Tarasevich, Am. Ceram. Bull. 63 (1985) 500.
12. J. Zarzycki, Heterogenious Chemistry Reviews 1 (1994) 243.
13. D. Porezag, Th. Frauenheim, Th. Köhler, G. Seifert, and R. Kaschner, Phys. Rev. B51 (1995) 12947.
14. T.W. Ebbesen and P.M. Ajayan, Nature 358 (1992) 220.
15. R. Gutierrez, Th. Frauenheim, Th. Köhler, and G. Seifert, J. Mater. Chem. 6 (1996) 1657.
16. R. Kaschner, Th. Frauenheim, Th. Köhler, and G. Seifert, J. Computer-Aided Mat. Design 4 (1997) 53.